



CHALMERS
UNIVERSITY OF TECHNOLOGY

The potential of magnetisation transfer NMR to monitor the dissolution process of cellulose in cold alkali

Downloaded from: <https://research.chalmers.se>, 2023-05-05 04:15 UTC

Citation for the original published paper (version of record):

Gunnarsson, M., Hasani, M., Bernin, D. (2019). The potential of magnetisation transfer NMR to monitor the dissolution process of cellulose in cold alkali. *Cellulose*, 26(18): 9403-9412. <http://dx.doi.org/10.1007/s10570-019-02728-y>

N.B. When citing this work, cite the original published paper.



The potential of magnetisation transfer NMR to monitor the dissolution process of cellulose in cold alkali

Maria Gunnarsson · Merima Hasani · Diana Bernin 

Received: 16 June 2019 / Accepted: 3 September 2019 / Published online: 12 September 2019
© The Author(s) 2019

Abstract Cellulose is the most important biopolymer on earth and, when derived from e.g. wood, a promising alternative to for example cotton, which exhibits a large environmental burden. The replacement depends, however, on an efficient dissolution process of cellulose. Cold aqueous alkali systems are attractive but these solvents have peculiarities, which might be overcome by understanding the acting mechanisms. Proposed dissolution mechanisms are for example the breakage of hydrophobic interactions and partly deprotonation of the cellulose hydroxyl groups. Here, we performed a mechanistic study using equimolar aqueous solutions of LiOH, NaOH and KOH to elucidate the dissolution process of microcrystalline cellulose (MCC). The pH was the highest

for KOH(aq) followed by NaOH(aq) and LiOH(aq). We used a combination of conventional and advanced solution-state NMR methods to monitor the dissolution process of MCC by solely increasing the temperature from -10 to 5 °C. KOH(aq) dissolved roughly 25% of the maximum amount of MCC while NaOH(aq) and LiOH(aq) dissolved up to 70%. Water motions on nanoscale timescales present in non-frozen water, remained unaffected on the addition of MCC. Magnetisation transfer (MT) NMR experiments monitored the semi-rigid MCC as a function of temperature. Interestingly, although NaOH(aq) and LiOH(aq) were able to dissolve a similar amount at 5 °C, MT spectra revealed differences with increasing temperature, suggesting a difference in the swollen state of MCC in LiOH(aq) already at -10 °C. Furthermore, MT NMR shows a great potential to study the water exchange dynamics with the swollen and semi-rigid MCC fraction in these systems, which might give valuable insights into the dissolution mechanism in cold alkali.

M. Gunnarsson · M. Hasani
Division of Forest Products and Chemical Engineering,
Department of Chemistry and Chemical Engineering,
Chalmers University of Technology,
SE-412 96 Gothenburg, Sweden

M. Hasani
Wallenberg Wood Science Center, The Royal Institute of
Technology, Chalmers University of Technology,
SE-100 44 Stockholm, Sweden

D. Bernin (✉)
Division of Chemical Reaction Engineering, Department
of Chemistry and Chemical Engineering, Chalmers
University of Technology, SE-412 96 Gothenburg,
Sweden
e-mail: diana.bernin@chalmers.se

Keywords Cellulose · Dissolution · Alkali · NMR · Magnetisation transfer · pH

Introduction

Dissolution of cellulose is an important process for the production of for example textile fibres, barriers, filters etc. The amphiphilic character of the polymer, which associates through both intra- and intermolecular hydrogen bonds and hydrophobic interactions, is though a limiting factor in finding solvents capable of dissolving cellulose (Lindman et al. 2010; Medronho et al. 2012; Medronho and Lindman 2014). A number of options have been reported to be efficient such as molten organic salts and aqueous complexing agents (Liebert 2010). The properties of the final cellulose-based product are highly dependent on the dissolution efficiency of cellulose on a molecular level, i.e. if the cellulose chains are aggregated, swollen or separated. One of the most environmentally friendly dissolution systems for cellulose, although not yet commercially implemented, is cold aqueous metal alkalis. The ability of NaOH(aq) to dissolve cellulose was found already in the beginning of the 1920's by Lilienfeld (1924) and was thereafter studied for several aqueous metal alkalis more in detail by Davidson (1934). Even though these solvent systems utilise chemicals familiar to the pulp and paper industry and therefore should be easy to implement in a commercial process, the problem of generating stable solutions has been a major obstacle. A stable solution refers to the ability of the cellulose chains to remain dissolved without any physical changes such as gelation or precipitation, and is a main criterion for the production of textile fibers and film to obtain high quality properties during coagulation of the dissolved cellulose chains. The reason for this instability is the narrow dissolution window at a specific concentration of NaOH(aq) and a certain temperature, namely around 2.0 M and $-5\text{ }^{\circ}\text{C}$ (Sobue et al. 1939). The ability to widen the dissolution window and thus maintain a more stable solution has been shown possible through the addition of for example urea, thiourea and ZnO (Cai and Zhang 2005; Yang et al. 2011; Zhou et al. 2004; Zhang et al. 2002). The complex, although fascinating, dissolution mechanism for cellulose in NaOH(aq) has still no definite explanation although many hypotheses have been developed, which includes partial deprotonation of the hydroxyl groups and hydration shells around the ions as driving forces (Bialik et al. 2016; Budtova and Navard 2016).

A comparison of the dissolution capacity of different aqueous metal alkalis based on wt% might be misleading, especially when combined with an additive based on wt% because the number of ionic species will differ. In addition, the properties of the solvent systems such as pH and activity coefficients might be different. Due to different pK_b 's of the aqueous metal alkalis, this is of special importance for concentrated solutions. Notably, the addition of urea was recently found to increase the pH of a NaOH(aq) (Gunnarsson et al. 2019). Hence, in order to draw valid conclusions towards a possible mechanism or mechanisms, careful considerations of how to compare these solvents are crucial.

Nevertheless, swelling is believed to be the first step to dissolution and the interaction with water during this process seems to play an important role (Budtova and Navard 2016). There is, however, a lack of experimental techniques to monitor the swelling of cellulose without disturbing the cellulose structure by shearing or filtering, a requirement for light scattering techniques. Hence, in this work, we compared the dissolution process of microcrystalline cellulose (MCC) in equimolar LiOH(aq), NaOH(aq) and KOH(aq) solutions at -10 , -5 and $5\text{ }^{\circ}\text{C}$ using NMR spectroscopy by solely increasing the temperature. The amount of dissolved cellulose was estimated from 1D ^1H NMR spectra and confirmed by ^{13}C NMR. Gustavsson et al. (2014) and Alves et al. (2016) employed recently polarisation transfer NMR from ^{13}C to ^1H to elucidate the solid and dissolved state of cellulose in various solvent systems, while we herein applied magnetisation transfer (MT) NMR to monitor the semi-rigid swollen cellulose and associated water exchange dynamics. We observed differences in MT spectra with increasing temperature and solvent system and want to highlight the potential of MT NMR to report on the swollen state of cellulose, which might give additional clues to understand the dissolution mechanism in cold aqueous alkali.

Materials and methods

Materials

Microcrystalline cellulose (MCC) Avicel PH-101, with a degree of polymerisation of 260, was purchased

from FMC BioPolymer and used without further treatment. LiOH (> 98%) and KOH (> 85%) were purchased from Merck. NaOH (< 98%) and D₂O (99.9%) were purchased from Sigma Aldrich. Urea (99%) was purchased from VWR. All chemicals were used without further purification.

Sample preparation

An appropriate amount of MCC to give in total 0.4 M was weighed into a 5 mm NMR tube and 500 μ L aqueous 2.0 M LiOH, NaOH, KOH or NaOH/2.5 M urea containing 80% D₂O was added on top. The mixture was then blended rigorously in the NMR tube during a couple of minutes using a vortex mixer until it appeared as a visually homogeneous suspension, i.e. when all MCC in the bottom of the NMR tube was observed as mixed with the solvent. The sample was immediately transferred to the freezer at -20°C and kept there until the start of the NMR experiments. The spectrometer was set to -15 or -10°C before inserting the NMR tube. Reference solutions were aqueous 2.0 M LiOH, NaOH or KOH without the addition of MCC.

pH

The pH measurements were carried out by pre-cooling the reference solutions with a concentration of 0.5 M at 10°C . The concentration was reduced to avoid exceeding the measurable maximum with our setup, which is 14, and compensate for the temperature dependency, which results in a larger pH with decreasing temperature. The pH was measured using a HACH HQ430D Multimeter with an Intellical PHC705A1 pH probe.

NMR

The NMR experiments were recorded on a 11.74 T (600 MHz) Bruker Avance III HD equipped with a diffusion probe fitted with a 5 mm ¹H radio frequency (RF) insert. The spin-lattice relaxation time T_1 was estimated from inversion-recovery experiments with 16 variable delays t from 0.1 up to 5 s and the spin-spin relaxation time T_2 from CPMG experiments with an echo spacing of 1.5 ms, resulting in the longest echo time et of 380 ms. The spin-lattice relaxation rates R_1

were calculated by $1/T_1$. The T_1 was obtained by regressing the signal intensity I versus t in each Fourier transformed point of the spectrum to $I = I_0(1 - a * \exp(-t/T_1))$ and for the T_2 versus et to $I = I_0 * \exp(-et/T_2)$ where I_0 is the non-weighted signal intensity at $t = 0$ or $et = 0$. a is a pre-exponential factor, which for an inversion-recovery sequence should be close to 2. We used a mono-exponential fitting albeit some signal decays or build-ups revealed a slightly curved decay in the semilogarithmic representation. Hence, the estimated relaxation times/rates represent mean values based on a cut-off of 0.94 for the ratio of the sum of squares of the regression and the total sum of squares.

1D ¹H spectra were recorded with a repetition delay of 20 s to enable a quantitative comparison. MT experiments were recorded with 128 frequency steps starting from -88.3 up to 83.3 ppm. Smaller steps were chosen close to the water peak and larger steps further away from the water peak. The duration of RF pulse for the saturation was 2 s with a B_1 field of 1580 Hz. A MT spectrum also denoted Z-spectrum represents the signal intensity of the water peak as a function of the saturation frequency in ppm. The intensity is normalised by the maximum intensity.

This setup of experiments were run at -15 ,¹ -10 , -5 and 5°C . After stabilisation of the set temperature, the sample was allowed to rest for additional 15 min prior to the start of the NMR experiments.

The 1D ¹³C NMR spectra experiments were recorded on an 18.8 T (800 MHz) magnet with a Bruker Avance III HD console and a TXO cryoprobe. The samples were prepared in the same manner as described above but in a 3 mm NMR tube. A single excitation pulse sequence with proton decoupling was applied with a repetition delay of 5 s.

Results and discussion

There has been large debate on possible dissolution mechanisms of cellulose in various solvent systems (Lindman et al. 2010). One of the hypotheses about the cold aqueous metal alkali system is that cellulose turns into a polyelectrolyte due to deprotonation of the hydroxyl groups on cellulose. Bialik et al. reported

¹ Only measured for a few samples.

recently on the partial deprotonation of the C2 carbon in cellobiose in this solvent using a combination of experimental ^1H and ^{13}C chemical shifts and DFT calculations (Bialik et al. 2016).

If deprotonation would be the sole mechanism for dissolution, the higher the pH of the solvent, the more efficient the dissolution of MCC would be. However, solutions at $> 0.1\text{ M}$ are inherently intricate because the concentration is beyond instrument limitations and applicable theories. Hence it is not obvious that a higher alkali concentration would lead to higher pH, greater deprotonation and/or the dissolution of cellulose, which is also described in the phase diagram by Sobue et al. (1939). Still, the pH of the solvent is of interest for the understanding of the dissolution mechanism of cellulose in aqueous metal alkalis as it reflects on the activity of H^+ and charges present in the system but has, to our knowledge, not been elaborated on yet. Thus, we here elucidated on the actual difference in pH of the three reference solutions LiOH(aq) , NaOH(aq) and KOH(aq) at equimolar concentration estimated to be within the detectable range of the pH electrode, namely 0.5 M at $10\text{ }^\circ\text{C}$, because pH is in addition temperature dependent. Although the alkali concentration and temperature are not equivalent to the conditions necessary for dissolution of cellulose, a relative comparison of the three solvents and their actual difference could provide valuable insight into the true solvent system.

Interestingly, the measurement showed that the pH of KOH(aq) was outside of the measurable region i.e. above 14 while the pH of LiOH(aq) and NaOH(aq) was 13.67 and 13.96, respectively (Table 1), which clearly describes the difference in activity of the three solvents. According to the CRC Handbook of Chemistry and Physics, the pK_a for Na^+ and Li^+ at $25\text{ }^\circ\text{C}$ is 14.8 and 13.8, respectively, which also further is in agreement with literature reporting on KOH being the

strongest base (Tata 1980). Although, the pH differences at 0.5 M are small, we want to stress that the pH at 2.0 M , a pre-requisite to dissolve cellulose, is close to the pK_a of the alkalis and MCC, at which small pH differences result in significant changes in the amount of charged species.

Taken together, deprotonation as the sole mechanism for dissolution of cellulose would from these results suggest KOH(aq) to be the best solvent for cellulose.

Dissolved cellulose

The normalised integrals of the MCC peak obtained from $1\text{D } ^1\text{H}$ NMR spectra established the contrary (Fig. 1). At $5\text{ }^\circ\text{C}$, KOH(aq) dissolved roughly 25% of the maximum amount of MCC (yellow dashed line), which is in accord with earlier reported results by Davidson (1937) but disagrees with results reported by Xiong et al. (2013) and Cai and Zhang (2005). In NaOH(aq) and LiOH(aq) , more than 70% MCC dissolved at $5\text{ }^\circ\text{C}$. This result is in agreement with the observations from Alves et al. (2016), who reported on a remaining solid MCC fraction in the NaOH(aq) system using 10% MCC while we used 6.5%. Furthermore, employing static light scattering

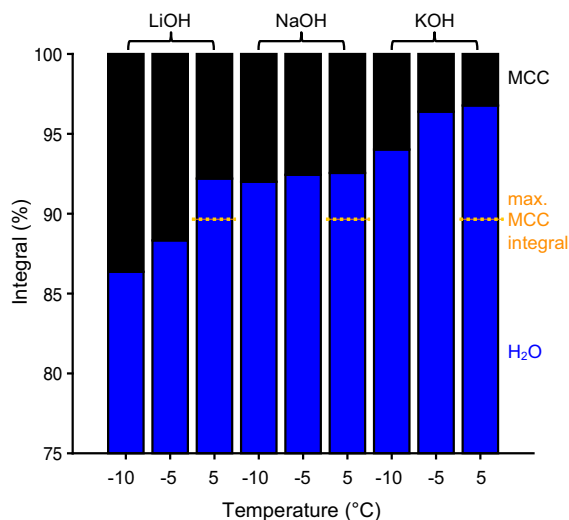


Fig. 1 Normalised integrals for MCC (black) and the water peak (blue) at -10 , -5 and $5\text{ }^\circ\text{C}$ estimated from $1\text{D } ^1\text{H}$ NMR spectra normalised by the total amount of signal. Highlighted in yellow (dashed line) is the maximum amount of dissolved MCC based on the known amounts of MCC

Table 1 The pH of aqueous reference alkali solutions at 0.5 M and $10\text{ }^\circ\text{C}$

Sample	pH
LiOH	13.67
NaOH	13.96
KOH	> 14

(Hagman et al. 2017), micrometer-sized aggregates were found when dissolving 1% MCC in NaOH(aq).

The observable ^1H signals arise from non-frozen and NMR-detectable water and dissolved MCC. A ^1H spectrum for LiOH(aq) with the addition of MCC recorded at 5 °C is shown in Fig. 6a. In this representation, the water peak was set to 0 ppm, which shifts the clearly visible MCC peaks to negative ppm values.

From Fig. 1, it appears that a larger amount of MCC dissolved in LiOH(aq) at both -10 and -5 °C compared to NaOH(aq) and KOH(aq) because the MCC integral (black) is larger. The mark (yellow dashed line) highlights the maximum MCC integral value corresponding to the dissolution of all added MCC. In case for LiOH(aq), the measured MCC integral of dissolved MCC exceeds the maximum amount at these temperatures. It is therefore suggested that this solvent, rather than being a better solvent for cellulose, has a lower amount of NMR-detectable H_2O , i.e. a lower amount of H_2O being non-frozen at -10 and -5 °C. LiOH(aq) has, however, a lower freezing point than both NaOH(aq) and KOH(aq) (Washburn 1926), which indicates that the addition of MCC impacts the freezing behaviour of water. This is further strengthened by the detected amount of dissolved MCC shown to decrease with temperature and at 5 °C passing the maximum amount mark. The same phenomenon of a decreasing amount of dissolved MCC at increased temperature could also be observed in KOH(aq), which is, however, more likely due to a decreasing dissolution capacity of the solvent with increasing temperature since KOH(aq) exhibits the lowest freezing-point depression of the three solvents. Interestingly, this was not the case for NaOH(aq) as the amount of dissolved MCC measured only changed slightly with increasing temperature, which could be an indication of the amount dissolved MCC and non-frozen H_2O changing simultaneously and that NaOH(aq) is a more effective solvent for cellulose within this temperature range in comparison to KOH(aq).

The NaOH(aq) solvent comprising in addition 2.5 M urea manifested a similar MCC integral at -15 , -5 and 5 °C as NaOH(aq) at all temperatures and LiOH(aq) at 5 °C due to the fact that this sample never froze at -20 °C (data not shown). Doubling the amount of MCC to 0.8 M in NaOH(aq) resulted in a MCC integral comparable to 0.4 M, which suggests

the system to be less effective at higher concentrations but this could also be an effect of the very high viscosity in this system that hampers the dissolved MCC to be detected (data not shown).

In addition, we recorded ^{13}C NMR spectra for MCC in LiOH(aq), NaOH(aq) and KOH(aq) at -5 and 5 °C, which enables the detection of each carbon in the MCC monomeric unit β -glucopyranoside (Fig. 2). These results match with the observations from the ^1H spectra although no efforts have been made to enable a quantitative comparison. The MCC peaks for LiOH(aq) (red) and NaOH(aq) (black) are equally strong at -5 and 5 °C while for KOH(aq), the peaks are barely visible, although present, which indicates a lower amount of MCC dissolved in KOH(aq). The ^{13}C signal intensity seems to increase with increasing temperature for LiOH(aq) and NaOH(aq), which is in agreement with the results obtained from the 1D integrals.

No external chemical shift reference could be used, which allows only a qualitative comparison of the chemical shift. However, the ^{13}C chemical shift observed in NaOH(aq) matched with the chemical shifts reported for dissolved cellulose in NaOH(aq) by Alves et al. (2016) but are for all carbons approximately 2 ppm lower compared to ^{13}C chemical shifts published by Isogai (1997), who studied MCC with DP 15 in 20% NaOH(aq) in comparison to 8%. There was a minor chemical shift change for position C6 with temperature to larger chemical shift values in LiOH(aq) and NaOH(aq) while the chemical shift values differed slightly for position C1, C2, C3, C5 and C6 in LiOH(aq) compared to NaOH(aq), which

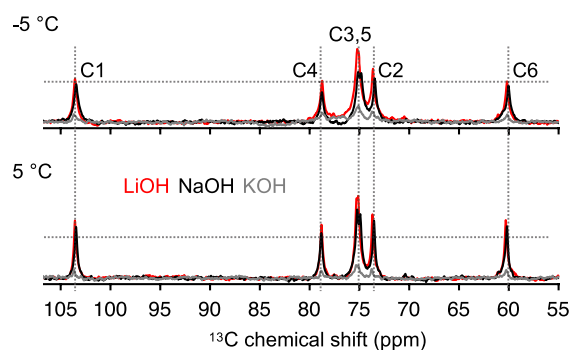


Fig. 2 1D non-scaled ^{13}C NMR spectra for MCC in LiOH(aq), NaOH(aq) and KOH(aq) recorded at -5 and 5 °C. The gray dashed lines are positioned at the same amplitude in both spectra and are a guide to the eye

suggests that the dissolved MCC is similar on an atomic level in all solvents.

Mean T_1 s for MCC and non-frozen water are converted to mean spin-lattice relaxation rates R_1 s by $1/T_1$. An Arrhenius plot showed that the mean spin-lattice relaxation rates R_1 of non-frozen water in LiOH(aq), NaOH(aq) and KOH(aq) followed a straight line (Fig. 3a). For LiOH(aq), the line manifested the steepest slope while for KOH(aq), the slope was the lowest. Interestingly, the Arrhenius behaviour for water was similar upon the addition of MCC. The observed temperature dependence for NaOH(aq) agrees with Yamashiki et al. (1988) although they reported on a stronger impact on R_1 upon the addition of cellobiose. The T_1 is sensitive to motions and fluctuations on the nanosecond timescale, which, when present, shorten the T_1 (Levitt 2008). However,

the addition of MCC seems to not impact the water motions in that regime.

Non-frozen water exhibited the longest T_1 in KOH(aq) and the shortest in LiOH(aq). For small molecules such as water, which are characterised by rotational correlation times of less than a 1 ns, T_1 increases and R_1 decreases with increasing temperature, which is in agreement with our findings. In contrast, the R_1 of the MCC arrived at a plateau at -5°C for the LiOH(aq), NaOH(aq), KOH(aq) and NaOH(aq) with 0.8 M MCC instead of 0.4 M (Fig. 3b). In addition, an already thawed NaOH(aq) system followed the trend for the measured temperatures, -15 and -5°C . For NaOH(aq)/2.5 M urea (gray), the plateau appeared to be below -15°C , which might be explained by this system still being liquid like at this temperature.

The parameter T_2 is instead an indicator of motions and fluctuations occurring on the millisecond timescale (Levitt 2008). Here, we normalised the mean T_2 of non-frozen water in LiOH(aq), NaOH(aq) and KOH(aq) with the addition of MCC by the mean T_2 of the reference solutions. For LiOH(aq), the normalised T_2 of water stayed constant while for KOH(aq) the normalised T_2 increased with temperature (Fig. 4, blue and black). The addition of MCC to KOH(aq) influenced the mean T_2 the most. The T_2 s are most likely affected by the exchange of the water molecules with the hydroxyl groups on the dissolved MCC and with the water that is associated with the semi-rigid MCC discussed in the next part. The mean

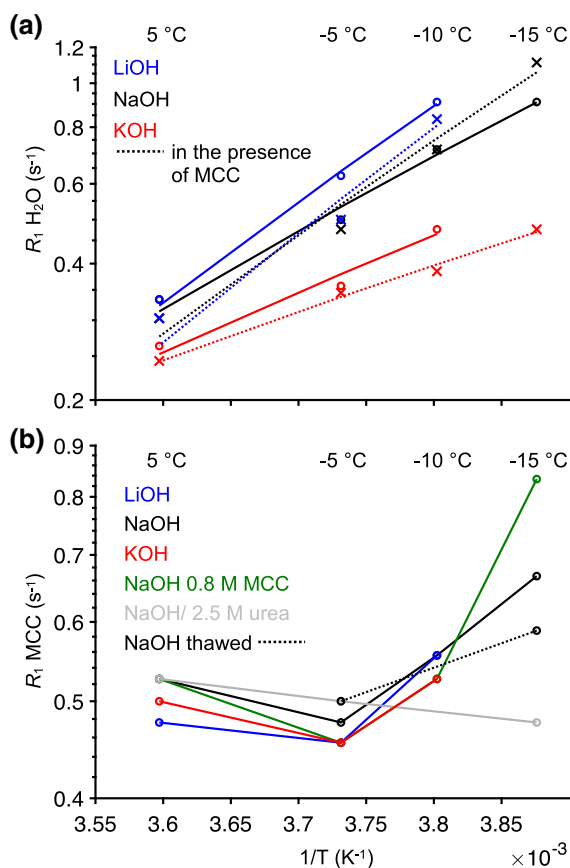


Fig. 3 Arrhenius plot of the mean R_1 of H_2O (a) and MCC (b) as a function of temperature. In a, the straight lines represent the data points fitted to a pseudo-Arrhenius behaviour while in b the lines are guides to the eye

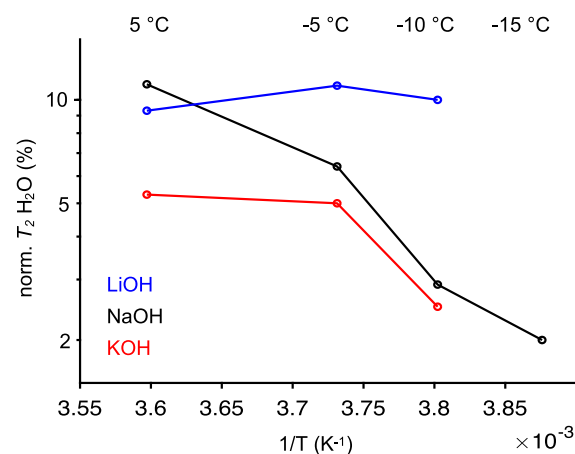


Fig. 4 Arrhenius plot of mean T_2 of H_2O in LiOH(aq) (blue), NaOH(aq) (black) and KOH(aq) (red) normalised by the T_2 of the reference solutions as a function of temperature

T_2 of the dissolved MCC is on the order of a couple of tens of milliseconds, hampering an accurate estimation.

Semi-rigid cellulose

In other research fields, magnetisation transfer (MT) NMR experiments have been used to estimate the exchange rates of H_2O with mobile/exchangeable protons present in OH- or NH_2 -groups, which resonate close to the water peak in a 1H NMR spectrum and are only visible when exchanging slower than approximately 100 Hz. Furthermore, MT NMR is able to observe protons associated to semi-rigid polymers or tissues, which are invisible for conventional 1H NMR due to their short T_2 s (Zaiss et al. 2015). Bulk water molecules exchanging with “bound and immobile” water molecules on semi-rigid cellulose are illustrated in Fig. 5. With “bound and immobile” water molecules, we mean water molecules that keep associated with the semi-rigid cellulose for timescales shorter than the exchange rate k_{off} . The invisible signal of “bound and immobile” water molecules and the semi-rigid cellulose might cover a ppm range of 10–150 ppm, too broad to be detected because of short T_2 s and homonuclear dipolar couplings, which might be up to 70 kHz. When irradiating the invisible signal, the “bound and immobile” water molecules will transfer their magnetisation to the bulk water molecules if there is an exchange not faster than approximately 10^3 Hz (Anthis and Clore 2015). As a result, the bulk water molecules become saturated and the intensity of the water peak will decrease.

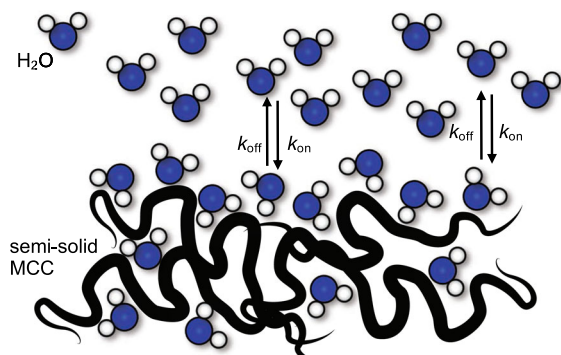


Fig. 5 Schematic illustration of “bound and immobile” water molecules to semi-rigid MCC exchanging with bulk water on the k_{on} and k_{off} timescale

Hence, an MT spectrum or a so called Z-spectrum displays the intensity of the water peak as a function of the irradiation frequency denoted offset as it is the frequency offset from the water peak, which is set to 0 ppm. A 1H NMR spectrum of LiOH(aq) with the addition of MCC at 5 °C is shown in Fig. 6a, where the water peak is set to 0 ppm. If there would be an exchange process occurring at a rate slower than approximately 10^3 Hz between water molecules and the hydroxyl groups of MCC, whose H1–H6 peaks resonate here at negative ppm values while the hydroxyl groups would appear at positive ppm values, the Z-spectrum would show a dip at the position where the exchange happens. We expect, however, the exchange rate at this high pH in alkali to be much faster (Zhou and van Zijl 2006), which explains why the Z-spectra lack these features (see Fig. 6b–d).

Instead, the Z-spectra showed different shapes and widths for LiOH(aq) (b), NaOH(aq) (c) and KOH(aq) (d) at -10 , -5 and 5 °C. The width, which we here attribute to the swollen state of semi-rigid MCC, depends mainly on the $1/T_2$ of the protons associated to the semi-solid fraction (Sled 2018). At -10 °C, the width was similarly broad for NaOH(aq) and KOH(aq) while for LiOH(aq), the width was much smaller suggesting that the semi-solid MCC is swollen to a greater extent for LiOH. The broadening of the curve started first above 0.2 of the normalised intensity, indicating that the fraction of semi-rigid MCC for LiOH(aq) is less compared to KOH(aq) and NaOH(aq). For LiOH(aq), the fraction rather than the width changed with temperature. A similar behaviour was found for KOH(aq) although the normalised intensity stayed constant when increasing the temperature from -5 to 5 °C. At 5 °C, there was still a broad feature visible, which agrees with the 1H integrals revealing a fraction of non-dissolved MCC with the largest fraction for KOH(aq). Interestingly, we observed a dip at above 60 ppm for all Z-spectra at -5 °C, which needs to be further investigated as no explanation was found here. For NaOH(aq), both normalised intensity and width changed with increasing temperature, which might indicate that the semi-rigid MCC swelled to a greater extent from -5 to 5 °C. This result might be related to the reported decrease of the intrinsic viscosity of cellulose in the NaOH(aq) system with increasing temperature (Roy et al. 2003; Kamide et al.

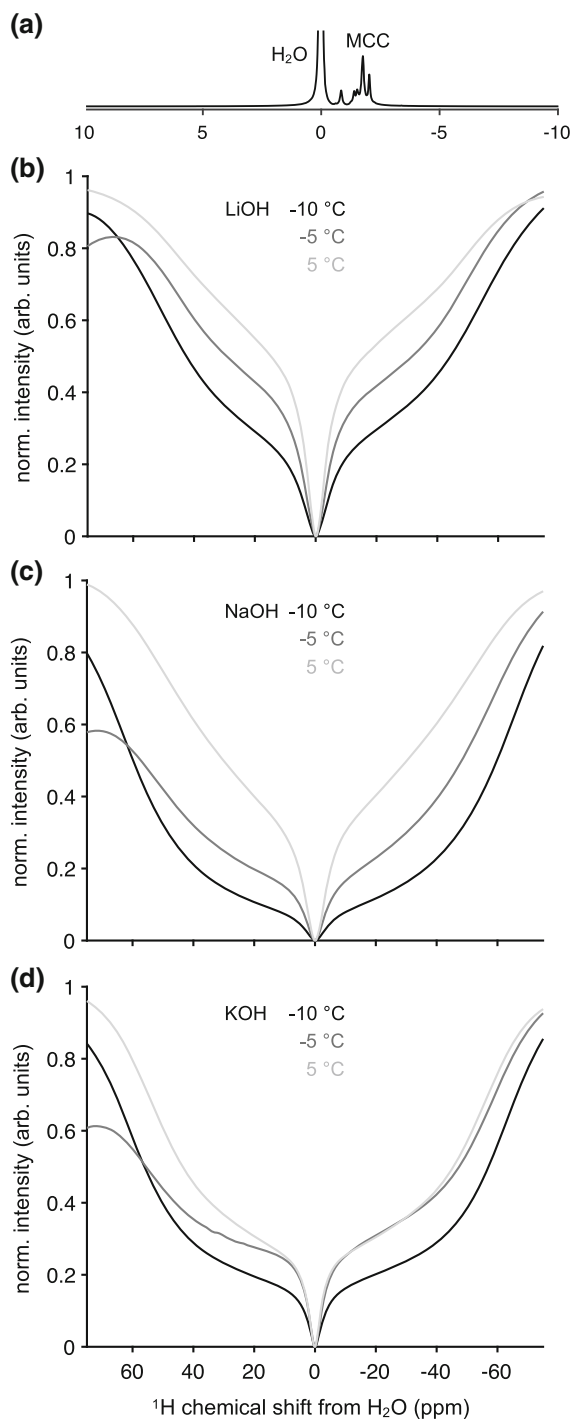


Fig. 6 1D ^1H spectrum of LiOH(aq) with the addition of MCC (a). MT (Z-)spectra for LiOH(aq) (b), NaOH(aq) (c) and KOH(aq) (d) as a function of temperature. The chemical shift scale is normalised to the water peak, which is set to 0 ppm

1987) although shearing might affect the cellulose structure.

In general, the shape and width of the Z-spectrum depends, however, on many parameters such as the exchange rate k_{on} and k_{off} as well as T_1 and T_2 of water and the semi-rigid MCC, the water and semi-rigid MCC fractions, the saturation duration and the B_1 field of the saturation RF pulse. Changing the saturation duration and B_1 field of the saturation would allow extracting k_{on} and k_{off} and details about the exchange of water molecules with the semi-rigid MCC and the semi-rigid MCC itself. We foresee that MT NMR could most likely contribute to elucidate recent modelling results such as if the concentration of water is higher around the hydroxyl groups (Stenqvist et al. 2015) or that there is more tightly coordinated water structure close to the microfibrillar cellulose chains (Hadden et al. 2013). However, this is out of the scope for this work and part of future studies. The clear distinction in dissolution capacity between NaOH(aq) and KOH(aq) falls in line with the phenomenon of a so-called reversed Hofmeister series (Sivan 2016). In the case of a normal Hofmeister series, ions of a certain bare ionic radius are considered as hydrophilic or hydrophobic. Li^+ and Na^+ are considered hydrophilic and strongly hydrated while K^+ is considered as hydrophobic and weakly hydrated. This means that when a hydrophobic surface, such as a hydrophobic surface of the amphiphilic cellulose, is introduced in the solvent, the more hydrophobic K^+ ion will accumulate on the surface to minimise its free energy while Li^+ and Na^+ remains associated with the solvent which is energetically the most favourable state for a hydrophilic ion. However, in the case of a reversed Hofmeister series, the hydrophobic surface is considered to be deprotonated due to an increase in pH, e.g. the hydroxyl groups on cellulose become deprotonated. Deprotonation of the surface increases its hydrogen bonding with H_2O , which in turn will lead to an expulsion of the K^+ ion from the surface as H_2O and strongly hydrated ions, such as Li^+ and Na^+ , minimise their free energy when binding to the surface (Sivan 2016). In other words, deprotonation in combination with sufficient binding of water, both by the cellulose and the ions present, could be an explanation for the difference in dissolution capacity of cold aqueous alkalis.

Conclusions

When comparing the dissolution process of MCC in equimolar solutions based on LiOH(aq), NaOH(aq) and KOH(aq), we found that KOH(aq) dissolved up to 25% of the maximum amount of MCC while LiOH(aq) and NaOH(aq) dissolved up to 70% without stirring. Fast bulk water dynamics were not affected by the addition of MCC. The spin-lattice relaxation rates of dissolved MCC as a function of temperature exhibited a plateau at $-5\text{ }^{\circ}\text{C}$ for all solvent systems except for NaOH/2.5 M urea, which revealed a plateau shifted to lower temperatures. MT NMR spectra reported on a different behaviour for the semi-rigid MCC when increasing temperature for LiOH(aq), NaOH(aq) and KOH(aq). The semi-rigid MCC appeared swollen to a greater extent for LiOH(aq) compared to KOH(aq) while for NaOH(aq) the swollen state changed from -5 to $5\text{ }^{\circ}\text{C}$. In conclusion, we present here an NMR methodology, which monitors water exchanges dynamics associated with the semi-rigid cellulose and the swollen state of the semi-rigid cellulose, which might play a crucial role for understanding the cellulose dissolution mechanism in cold aqueous alkali. To gain further insight, MT parameters need to be varied in a systematic matter, which is out of the scope of this work.

Acknowledgments Open access funding provided by Chalmers University of Technology. This work has been carried out as a part of the framework of Avancell - Center for Fiber Engineering, which is a research collaboration between Södra Innovation and Chalmers University of Technology. The author thanks the Södra Skogsägarnas Foundation for Research, Development and Education for their financial support. The Swedish NMR Center is acknowledged for spectrometer time.

Compliance with ethical standards

Conflict of interest The authors declare that they have no conflict of interest.

Open Access This article is distributed under the terms of the Creative Commons Attribution 4.0 International License (<http://creativecommons.org/licenses/by/4.0/>), which permits unrestricted use, distribution, and reproduction in any medium, provided you give appropriate credit to the original author(s) and the source, provide a link to the Creative Commons license, and indicate if changes were made.

References

- Alves L, Medronho B, Antunes FE, Topgaard D, Lindman B (2016) Dissolution state of cellulose in aqueous systems. 1. Alkaline solvents *Cellul* 23(1):247–258. <https://doi.org/10.1007/s10570-015-0809-6>
- Anthis NJ, Clore GM (2015) Visualizing transient dark states by NMR spectroscopy. *Q Rev Biophys* 48(1):35–116. <https://doi.org/10.1017/S0033583514000122>
- Bialik E, Stenqvist B, Fang Y, Östlund Å, Furó I, Lindman B, Lund M, Bernin D (2016) Ionization of cellobiose in aqueous alkali and the mechanism of cellulose dissolution. *J Phys Chem Lett* 7(24):5044–5048. <https://doi.org/10.1021/acs.jpclett.6b02346>
- Budtova T, Navard P (2016) Cellulose in NaOH-water based solvents: a review. *Cellulose* 23(1):5–55. <https://doi.org/10.1007/s10570-015-0779-8>
- Cai J, Zhang L (2005) Rapid dissolution of cellulose in LiOH/urea and NaOH/urea aqueous solutions. *Macromol Biosci* 5(6):539–548. <https://doi.org/10.1002/mabi.200400222>
- Davidson G (1937) The dissolution of chemically modified cotton cellulose in alkaline solutions. Part 3—In solutions of sodium and potassium hydroxide containing dissolved zinc, beryllium and aluminium oxides. *J Text Inst Trans* 28(2):T27–T44. <https://doi.org/10.1080/19447023708631789>
- Davidson GF (1934) The dissolution of chemically modified cotton cellulose in alkaline solutions. Part I—In solutions of sodium hydroxide, particularly at temperatures below the normal. *J Text Inst Trans* 25(5):T174–T196. <https://doi.org/10.1080/19447023408661621>
- Gunnarsson M, Bernin D, Hasani M (2019) Capturing of CO₂ in NaOH(aq) in the presence of urea and methyl β -glucopyranoside. Manuscript submitted for publication
- Gustavsson S, Alves L, Lindman B, Topgaard D (2014) Polarization transfer solid-state NMR: a new method for studying cellulose dissolution. *RSC Adv* 4(60):31836–31839. <https://doi.org/10.1039/C4RA04415K>
- Hadden JA, French AD, Robert J, Rj Woods (2013) Unraveling cellulose microfibrils: a twisted tale. *Biopolymers* 10:746–756
- Hagman J, Gentile L, Moestrup Jessen C, Behrens M, Bergqvist KE, Olsson U (2017) On the dissolution state of cellulose in cold alkali solutions. *Cellulose* 24:2003–2015
- Isogai A (1997) NMR analysis of cellulose dissolved in aqueous NaOH solutions. *Cellulose* 4(2):99–107. <https://doi.org/10.1023/A:1018471419692>
- Kamide K, Saito M, Kowsaka K (1987) Temperature dependence of limiting viscosity number and radius of gyration for cellulose dissolved in aqueous 8% sodium hydroxide solution. *Polym J* 19:1173–1181
- Levitt M (2008) Spin dynamics: basics of nuclear magnetic resonance, 2nd edn
- Liebert T (2010) Cellulose solvents—remarkable history, bright future. In: *Cellulose solvents: for analysis, shaping and chemical modification*, chap 1, pp 3–54. <https://doi.org/10.1021/bk-2010-1033.ch001>
- Lilienfeld L (1924) Manufacture of cellulose solution. British patent no. 212864

- Lindman B, Karlström G, Stigsson L (2010) On the mechanism of dissolution of cellulose. *J Mol Liq* 156(1):76–81. <https://doi.org/10.1016/j.molliq.2010.04.016>
- Medronho B, Lindman B (2014) Competing forces during cellulose dissolution: from solvents to mechanisms. *Curr Opin Colloid Interface Sci* 19(1):32–40. <https://doi.org/10.1016/j.cocis.2013.12.001>
- Medronho B, Romano A, Miguel M, Stigsson L, Lindman B (2012) Rationalizing cellulose (in)solubility: reviewing basic physicochemical aspects and role of hydrophobic interactions. *Cellulose* 19(3):581–587. <https://doi.org/10.1007/s10570-011-9644-6>
- Roy C, Budtova T, Navard P (2003) Rheological properties and gelation of aqueous cellulose NaOH solutions. *Biomacromolecules* 4(2):259–264. <https://doi.org/10.1021/bm020100s>
- Sivan U (2016) The inevitable accumulation of large ions and neutral molecules near hydrophobic surfaces and small ions near hydrophilic ones. *Curr Opin Colloid Interface Sci* 22:1–7. <https://doi.org/10.1016/j.cocis.2016.02.004>
- Sled JG (2018) Modelling and interpretation of magnetization transfer imaging in the brain. *Neuroimage* 182:128–135. <https://doi.org/10.1016/j.neuroimage.2017.11.065>
- Sobue H, Kiessig H, Hess K (1939) The system: cellulose-sodium hydroxide-water in relation to the temperature. *Z Physik Chem B* 43:309–328
- Stenqvist B, Wernersson E, Lund M (2015) Cellulose-water interactions: effect of electronic polarizability. *Nord Pulp Pap Res J* 30:26–31
- Tata GM (1980) Theoretical principles of inorganic chemistry. McGraw-Hill Education
- Washburn EW (1926) Freezing-point lowering of aqueous solutions. Knovel
- Xiong B, Zhao P, Cai P, Zhang L, Hu K, Cheng G (2013) NMR spectroscopic studies on the mechanism of cellulose dissolution in alkali solutions. *Cellulose* 20(2):613–621. <https://doi.org/10.1007/s10570-013-9869-7>
- Yamashiki T, Kamide K, Okajima K, Kowsaka K, Matsui T, Fukase H (1988) Some characteristic features of dilute aqueous alkali solutions of specific alkali concentration (2.5 mol L^{-1}) which possess maximum solubility power against cellulose. *Polym J* 20(6):447–457. <https://doi.org/10.1295/polymj.20.447>
- Yang Q, Qi H, Lue A, Hu K, Cheng G, Zhang L (2011) Role of sodium zincate on cellulose dissolution in NaOH/urea aqueous solution at low temperature. *Carbohydr Polym* 83(3):1185–1191. <https://doi.org/10.1016/j.carbpol.2010.09.020>
- Zaiss M, Zu Z, Xu J, Schuenke P, Gochberg DF, Gore JC, Ladd ME, Bachert P (2015) A combined analytical solution for chemical exchange saturation transfer and semi-solid magnetization transfer. *NMR Biomed* 28(2):217–230. <https://doi.org/10.1002/nbm.3237>
- Zhang L, Ruan D, Gao S (2002) Dissolution and regeneration of cellulose in NaOH/thiourea aqueous solution. *J Polym Sci Part B Polym Phys* 40(14):1521–1529. <https://doi.org/10.1002/polb.10215>
- Zhou J, van Zijl PCM (2006) Chemical exchange saturation transfer imaging and spectroscopy. *Prog Nucl Magn Reson Spectrosc* 48(2):109–136. <https://doi.org/10.1016/j.pnmrs.2006.01.001>
- Zhou J, Zhang L, Cai J (2004) Behavior of cellulose in NaOH/Urea aqueous solution characterized by light scattering and viscometry. *J Polym Sci Part B Polym Phys* 42(2):347–353. <https://doi.org/10.1002/polb.10636>

Publisher's Note Springer Nature remains neutral with regard to jurisdictional claims in published maps and institutional affiliations.